Polarization Instabilities in a Two-Photon Laser

Olivier Pfister,* William J. Brown,† Michael D. Stenner, and Daniel J. Gauthier‡

Department of Physics and Center for Nonlinear and Complex Systems, Duke University, Durham, North Carolina 27708-0305

(Received 24 December 2000)

We describe the operating characteristics of a new type of quantum oscillator that is based on a two-photon stimulated emission process. This two-photon laser consists of spin-polarized and laser-driven ^{39}K atoms placed in a high-finesse transverse-mode-degenerate optical resonator and produces a beam with a power of $\sim 0.2\ \mu$W at a wavelength of 770 nm. We observe complex dynamical instabilities of the state of polarization of the two-photon laser, which are made possible by the atomic Zeeman degeneracy. We conjecture that the laser could emit polarization-entangled twin beams if this degeneracy is lifted.

DOI: 10.1103/PhysRevLett.86.4512 PACS numbers: 42.50.Gy, 42.50.Dv, 42.65.Sf

The high degree of temporal coherence of laser light arises from a complex interplay between the fundamental light-matter interactions of absorption, spontaneous emission, and stimulated emission. The coherence properties of the generated light, characterized by the temporal coherence function, can be altered significantly and often in a surprising manner when quantum or nonlinear optical effects are paramount. For example, the threshold, stability, and quantum statistical properties of a single-atom maser [1] or laser [2] operating in the "cavity quantum electrodynamics regime" are very different from their multiatom counterparts. The coherence properties of laser light can also be modified by exploiting different types of light-matter interactions. For example, the two-photon laser [3,4] is based on the higher-order two-photon stimulated emission process, whereby two incident photons stimulate an excited atom to a lower energy state and four photons are scattered, as shown schematically in Fig. 1(a). This contrasts all other "standard" lasers that are based on the one-photon stimulated emission process whereby one photon stimulates an excited atom to a lower energy state and two photons are scattered.

While replacing the standard one-photon stimulated emission process by a high-order one might be expected to give rise to subtle differences observable only at the quantum level [5], it has been predicted that there will be dramatic changes in both the microscopic [6] and macroscopic laser behavior even when many atoms participate in the lasing process [7]. The reason for these differences is that the two-photon stimulated emission rate depends quadratically on the incident photon flux, resulting in an inherently nonlinear light-matter interaction.

As an example, consider the effects of such a nonlinearity on the threshold behavior of the two-photon laser. Briefly, the threshold condition for all lasers is that the round-trip gain must equal the round-trip loss. For one-photon lasers this yields the well known result that lasing will commence when a uniquely defined minimum inversion density (proportional to the gain) is attained via sufficient pumping. The situation is more complicated for the two-photon laser because the unsaturated gain increases with increasing inversion density *and* with increasing cavity photon number. This results in a threshold condition specified by a uniquely defined minimum inversion density and cavity photon number [8] so that it cannot turn on unless quantum fluctuations [9] or an injected field [4,8] brings the intracavity light above the critical value. In addition, once the minimum photon number exists in the cavity, the photon number undergoes a runaway process, growing rapidly until the two-photon transition is saturated [8]. Therefore, the two-photon laser operates in the saturated regime (a source of optical nonlinearity) even at the laser threshold, giving rise to the possibility that the laser will display dynamical instabilities.

The primary purpose of this paper is to present experimental observations of degenerate two-photon optical lasing that is based on laser-driven potassium atoms [10] contained in a very high-finesse optical resonator. We verify that the laser displays the expected turn-on behavior and observe that it displays polarization instabilities. Such experiments provide a window into the often conflicting predictions concerning two-photon lasers and will help identify generic two-photon laser properties. In addition, we suggest that this two-photon laser could emit polarization-entangled light states of interest for quantum information applications.

Achieving two-photon lasing is hampered by the smallness of typical two-photon stimulated emission rates and high saturation intensities, and competing nonlinear optical processes often swamp or prevent the occurrence of two-photon lasing. To overcome these difficulties, we follow the general approach [4] of using laser-driven

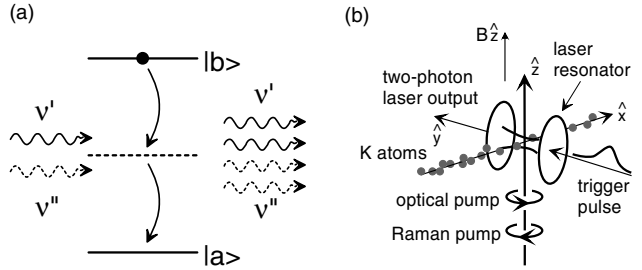

FIG. 1. (a) The idealized two-photon stimulated emission process. (b) Two-photon laser experimental setup.

 0031-9007/01/86(20)/4512(4)$15.00

interactions to generate the two-photon gain, and high-quality laser mirrors (developed for cavity quantum electrodynamics experiments [11]) for the optical resonator, as described below.

The two-photon gain medium we use in the experiments consists of a dense, collimated, effusive beam of laser-driven ^{39}K atoms that passes through the center of the optical resonator orthogonal to the resonator axis, as shown schematically in Fig. 1(b). We use the D_1 transition of ^{39}K (6 MHz natural linewidth) whose Zeeman hyperfine structure is displayed in Fig. 2. The atomic states are denoted by $|\alpha F_\alpha M_\alpha\rangle$, with $\alpha = g$ for $4^2S_{1/2}$ and $\alpha = e$ for $4^2P_{1/2}$ levels. Quantum numbers F and M denote the total angular momentum and its projection on the quantization axis $\hat{z}$, defined by a weak magnetic field ($\leq$1 G) produced by a small Helmholtz coil set around the cavity. The two-photon stimulated emission rate is enhanced by the smallness of the ground state hyperfine splitting for ^{39}K of $\Delta_g/2\pi = 462$ MHz. To create a population inversion for multiphoton transitions starting from the state $|g22\rangle$, the atoms are continuously optically pumped into this state by two $\hat{\sigma}_+$-polarized fields whose frequencies are set close to ω_{21} and ω_{22} (Bohr frequencies are denoted by $\omega_{F_eF_g}$). We note that the homogeneous linewidth of the Raman two-photon transition is $\approx$6 MHz due to lifetime broadening of the states by the optical pumping beams. The maximum atomic number density in the resonator is $\sim 2 \times 10^{11}$ atoms/cm^3, the atomic beam diameter is 2.5 mm, and the measured residual Doppler absorption width is 30 MHz.

The two-photon laser resonator is placed in a vacuum chamber and consists of two high-reflectivity ultra-low-loss mirrors of radius of curvature $R = 5$ cm set close together at a distance of $L = 1.464$ cm in a linear (standing-wave) transverse-mode-degenerate sub-confocal configuration. This configuration suppresses normal one-photon lasing that can arise from spectrally nearby gain features [10]. The laser mirrors are mounted on a superinvar structure to minimize thermal drift of L, with one mirror attached to a mount actuated by three "picomotors" (New Focus MRA 8302) to permit cavity alignment in vacuum and the other mirror is mounted on a piezoelectric ceramic for fine scanning L. The mirrors have a transmissivity of $T = 2 \times 10^{-4}$ as measured by the manufacturer (Research Electro-Optics). We find that the cavity finesse $\mathcal{F} = 15\,400 \pm 150 \simeq \pi/(T + A)$ using the ringdown technique, yielding a loss per mirror $A = (4 \pm 2) \times 10^{-6}$.

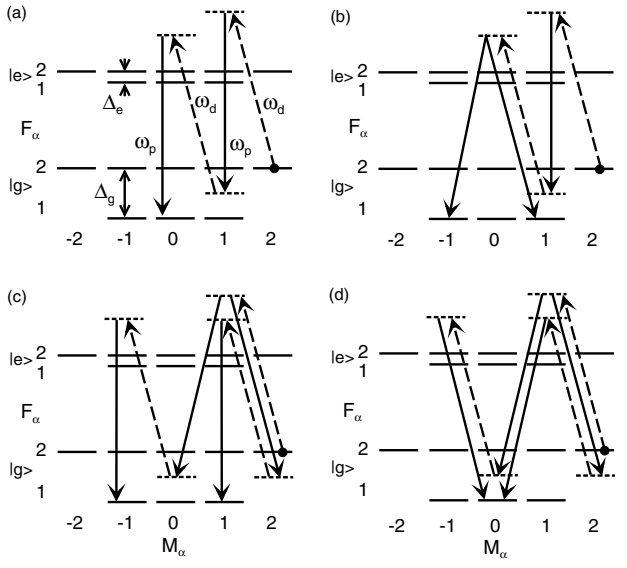

FIG. 2. Two-photon Raman scattering diagrams showing the quantum pathways for the possible states of polarization of the two-photon laser field (solid line) and the cicularly polarized Raman pump beam (dashed line).

We use a short cavity length so that the free spectral range (FSR $= c/2L = 10.24$ GHz) is larger than the frequency difference between the two-photon gain feature and all other nearby one-photon gain features, which are within 400 MHz of the two-photon frequency. We set the cavity length precisely to a subconfocal condition $L = R[1 \pm \cos(\pi/p)]$ with $p = 4$ so that the transverse modes group into degenerate clusters, spaced by $c/2pL = 2.56$ GHz and centered on the longitudinal mode frequencies. Finally, to suppress one-photon lasing on high-order transverse modes (which are no longer frequency degenerate with the lower-order modes due to spherical aberrations [12]), we accurately position under vacuum 400 μm pinholes in front of each cavity mirror and along the cavity axis using picomotor-actuated translation stages. With the pinholes in place, $\mathcal{F} = 15\,140$, resulting in a longitudinal mode linewidth FSR$/\mathcal{F} = 680$ kHz. Within the cavity mode volume, we estimate that there are a maximum of 7×10^6 atoms.

Two-photon stimulated emission into the laser cavity mode (frequency ω_l) occurs when the optically pumped atoms are illuminated by an intense $\hat{\sigma}_-$-polarized Raman pump beam of frequency ω_d, and ω_l is adjusted to the two-photon transition frequency ($\simeq \omega_d + \Delta_g/2$). Photons are added two at a time to the cavity field via stimulated emission when two photons are annihilated from the $\hat{\sigma}_-$-polarized Raman pump field and the atom undergoes a multiphoton transition from the state $|g22\rangle$ to any one of the states $|g1M_g\rangle$, as shown in Fig. 2. Note that such a hyper-Raman transition can be mapped onto the idealized two-photon stimulated emission process shown in Fig. 1(a) by working in a basis in which the multilevel atomic structure is dressed by the Raman pump field. The Raman pump beam has a maximum power of 300 mW and is focused to an elliptical spot size ($1/e$ field radius) of 3 mm along the cavity axis and 250 μm along the atomic beam axis, achieving a maximum intensity of approximately 25 W/cm^2. Throughout the experiments, the pump beam frequency is adjusted so that it is tuned to the blue side of the ω_{22} transition by 512 MHz. The mutually orthogonal geometry of our experiment suppresses

competing phase-matched processes, ensuring that we are constructing a true two-photon laser and not a parametric oscillator.

Our experimental system is very rich because there are four quantum pathways, depicted in Fig. 2, that connect the initial state $|g22\rangle$ and the final states $|g1M_g\rangle$, differ only by the state of polarization of the cavity field, and are frequency degenerate at zero magnetic field. The two-photon resonator can support any state of polarization (it is measured to be highly isotropic); hence all pathways of Fig. 2 must be considered.

Experimental evidence for the initiation of two-photon lasing is presented in Fig. 3, obtained using the following procedure. The atomic, optical pumping, and Raman pump beam are turned on and a weak tunable continuous-wave $\hat{z}$-polarized laser beam, produced by an auxiliary laser, is injected into the two-photon laser resonator. The frequency of the injected beam is scanned repeatedly through the cavity resonance while monitoring the power emanating from the cavity, and the cavity frequency is manually adjusted around the vicinity of the expected two-photon transition frequency ($\omega_l \simeq \omega_d + \Delta_g/2$).

In an attempt to force the laser to the "on" state, we typically inject a 1.2-μs-long pulse of light into the resonator, which is gated from the auxiliary laser beam using an acousto-optic modulator. Figure 3(a) shows the case when a below-threshold pulse is injected into the resonator. The dashed vertical lines indicate the duration of the injected pulse and we estimate that $n_{\text{inj}} = 1.1 \times 10^5$ photons are injected into the cavity. For slightly higher trigger pulse powers [Fig. 3(b), $n_{\text{inj}} = 2.2 \times 10^5$], the cavity photon number grows substantially and remains high for a few microseconds but is still insufficient to initiate lasing. The fact that the photon number stays high for a duration much longer than the pulse width indicates that we are very close to satisfying both two-photon laser threshold criteria. For $n_{\text{inj}} = 3.3 \times 10^5$ [Fig. 3(c)], the power emitted by the cavity rises to approximately 0.2 μW and remains at this value, corresponding to an average cavity photon number of 2.2×10^6 and an intracavity intensity of 7.3 W/cm^2 at the cavity waist. We observe that the power emitted from the cavity remains high for up to a few seconds until the frequency of the Raman pump or the cavity drifts off the two-photon resonance or the Raman pump beam is blocked momentarily. Figure 3(d) shows the power emitted from the resonator on a longer time scale for a larger injected number of photons and during a different experimental run but under essentially identical conditions. The experimental data of Fig. 3 give convincing evidence that we have indeed observed two-photon lasing.

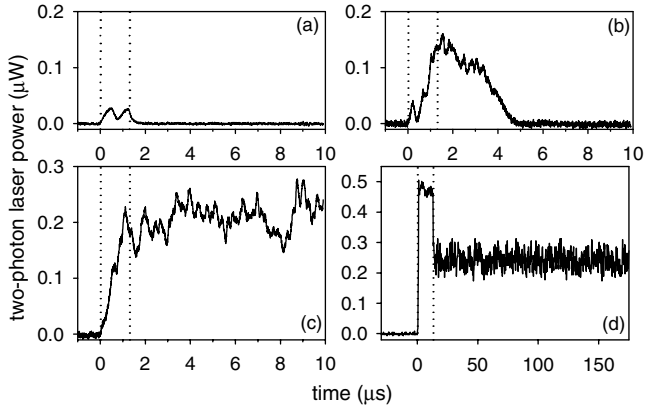

FIG. 3. Triggering the Raman two-photon laser by injecting an external pulse. In (a) and (b), the injected field is not strong enough to drive the laser to the high-power ("on") state.

As mentioned earlier, the degenerate hyperfine structure of ^{39}K opens up the possibility that the laser can operate on different states of polarization. Recall that we trigger the laser to the on state using a $\hat{z}$-polarized beam. To gain some understanding of the subsequent state of polarization, we place a linear polarizer oriented in the $\hat{z}$ direction in the beam and before the detector. We find that the two-photon laser displays polarization instabilities even though the total emitted power remains nearly constant on the time scale of the instability. It is seen in Fig. 4(a) that the state of polarization undergoes very regular oscillations of period 0.11 μs, with a 50% depth of modulation. Similar dynamical behavior is observed for all polarizer orientations, suggesting that the state of polarization is elliptical with an ellipticity of 0.5 and a rotating major axis. Additional experiments using multiple detectors to simultaneously record the power emitted in different states of polarization are needed to accurately quantify the laser's polarization state.

We find that the laser dynamics is quite sensitive to the applied magnetic field: an increase by as little as 0.5 G is sufficient to generate a much more complicated pattern. Figure 4(b) shows the complex, possibly chaotic behavior observed for a magnetic field strength of 2.0 G. An analysis of the data shown in Fig. 4(b) during the interval after which the injected pulse is turned off reveals that the irregular oscillations are characterized by a broad power spectrum and a correlation function that drops to near zero within 100 ns, necessary but not sufficient conditions for the existence of chaotic oscillations. Determining whether the oscillations are chaotic will require a much longer data set analyzed using nonlinear dynamics methods [13].

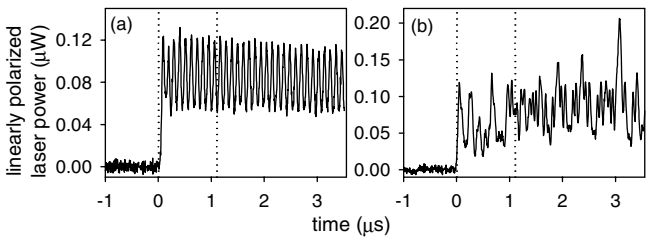

FIG. 4. Polarization instabilities in the Raman two-photon laser for (a) a weak and (b) a strong magnetic field.

The observation of instabilities in the Raman two-photon laser is surprising. Theoretical models of generic two-photon lasers, based on simplified energy level schemes, predict that the laser should be stable in the so-called "good cavity limit" [7]. Our experiment is carried out in this regime, where the cavity linewidth is narrower than, but comparable to, the population and atomic coherence linewidths. We suggest three possible mechanisms that may be responsible for the observed instability. One mechanism arises from the multiple frequency-degenerate final lasing states. As the laser turns on and begins to saturate the pathway shown in Fig. 2(a) (because we inject a $\hat{z}$-polarized trigger field), an $\hat{x}$-polarized field can begin to grow on the unsaturated pathways shown in Figs. 2(b) and 2(c) (that is enhanced by the existing $\hat{z}$-polarized cavity field). We note the one-photon lasers with a continuously injected signal [14] or with vector degrees of freedom can exhibit instabilities even in the good cavity limit [15].

Another possible mechanism is that the lasing takes place on multiple non-frequency-degenerate transverse modes arising from cavity mirror birefringence, for example. We do not believe that this is likely because of the following: we observe that a linearly polarized laser beam passing through the cavity in the absence of atoms remains linear to within our measurement sensitivity (one part in 10^5) for various input states of polarization, the transverse profile of the laser beam appears to be a lowest order TEM_{00} mode as measured by a video camera, and the pinholes placed in the cavity suppress all but the lowest-order transverse modes (we estimate the diffraction loss of the TEM_{01} mode of the empty cavity due to the pinholes is about a factor of 10 greater than the loss of the TEM_{00} mode [16]). Additional high-speed measurements of the spatial-temporal behavior of the beam profile will be needed to completely rule out the presence of transverse-mode instabilities.

Finally, the presence of standing waves may induce the instabilities; it is well known that counterpropagating laser beams in conjunction with a tensor nonlinear optical interaction can give rise to polarization instabilities with a reduced instability threshold [17]. Distinguishing between the first and the third mechanisms and possibly suppressing the instabilities should be possible using a stronger magnetic field to lift the degeneracy of the different quantum pathways.

Lifting the degeneracy between the pathways also has the promise of yielding polarization entanglement. Consider, for simplicity, a single emission event. When the Zeeman levels are degenerate, as in Fig. 2, the superposition of all possible amplitudes gives a photon pair $(1,2)$ in the state $[\alpha_1|\hat{z}\rangle_1 + \beta_1|\hat{x}\rangle_1][\alpha_2|\hat{z}\rangle_2 + \beta_2|\hat{x}\rangle_2]$ with $|\alpha_i^2| + |\beta_i^2| = 1$, where $|\hat{\varepsilon}\rangle_i$ $(\varepsilon = x, y)$ is the polarization-labeled Fock state of the ith photon of the emitted pair. In a strong magnetic field, the $\hat{x}\hat{z}$ and $\hat{z}\hat{x}$ pairs become off resonant and should stop lasing, creating the polarization-entangled state $\alpha_1\alpha_2|\hat{z}\rangle_1|\hat{z}\rangle_2 + \beta_1\beta_2|\hat{x}\rangle_1|\hat{x}\rangle_2$. Maximal entanglement $(\alpha_1\alpha_2 = \beta_1\beta_2)$ can be achieved by varying the resonant enhancement of a pathway, e.g., varying the Raman pump's frequency and power, and the magnetic field.

This work is supported by NSF Grant No. PHY-9876988.

*Present address: Department of Physics, University of Virginia, 382 McCormick Road, Charlottesville, VA 22904-4714.
†Present address: Corvis Corp., 7015 Albert Einstein Drive, Columbia, MD 21046-9400.
‡Corresponding author.
Email address: gauthier@phy.duke.edu

[1] D. Meschede, H. Walter, and G. Muller, Phys. Rev. Lett. **54**, 551 (1985).
[2] K. An, J. J. Childs, R. R. Dasari, and M. S. Feld, Phys. Rev. Lett. **73**, 3375 (1994).
[3] A. M. Prokhorov, Science **10**, 828 (1965); P. P. Sorokin and N. Braslau, IBM J. Res. Dev. **8**, 177 (1964); R. Z. Garwin, *ibid.* **8**, 338 (1964).
[4] D. J. Gauthier, Q. Wu, S. E. Morin, and T. W. Mossberg, Phys. Rev. Lett. **68**, 464 (1992).
[5] H. P. Yuen, Phys. Rev. A **13**, 2226 (1976); L. A. Lugiato and G. Strini, Opt. Commun. **41**, 374 (1982); M. D. Reid and D. F. Walls, Phys. Rev. A **28**, 332 (1983).
[6] See, for example, S. Bay, M. Elk, and P. Lambropoulos, J. Phys. B **28**, 5359 (1995); A. W. Boone and S. Swain, Phys. Rev. A **41**, 343 (1990); Y. Zhu and M. O. Scully, *ibid.* **38**, 5433 (1988); Y. Zhu and X. S. Li, *ibid.* **36**, 3889 (1987).
[7] See, for example, V. Espinosa, R. Vilaseca, E. Roldán, and G. J. de Valcárcel, Opt. Commun. **174**, 195 (2000); G. J. de Valcárcel, E. Roldán, J. F. Urchueguía, and R. Vilaseca, Phys. Rev. A **52**, 4059 (1995); J. Zakrzewski and M. Lewenstein, *ibid.* **45**, 2057 (1992).
[8] H. M. Concannon and D. J. Gauthier, Opt. Lett. **19**, 472 (1994); C. Z. Ning and H. Haken, Z. Phys. B **77**, 157 (1989).
[9] M. Brune, J. M. Raimond, P. Goy, L. Davidovich, and S. Haroche, Phys. Rev. Lett. **59**, 1899 (1987).
[10] O. Pfister, W. J. Brown, M. D. Stenner, and D. J. Gauthier, Phys. Rev. A **60**, R4249 (1999).
[11] G. Rempe, R. J. Thompson, H. J. Kimble, and R. Lalezari, Opt. Lett. **17**, 363 (1992); K. An, Y. Changhuei, R. R. Dasari, and M. S. Feld, Opt. Lett. **20**, 1068 (1995).
[12] M. Hercher, Appl. Opt. **7**, 951 (1968).
[13] H. D. I. Abarbanel, Rev. Mod. Phys. **65**, 1331 (1993).
[14] J. F. Urchueguía, V. Espinosa, and G. J. de Valcárcel, J. Mod. Opt. **46**, 1483 (1999).
[15] Yu. V. Loiko, A. M. Kul'minskii, and A. P. Voitovich, J. Opt. Soc. Am. B **17**, 1841 (2000).
[16] T. Li, Bell Syst. Tech. J. **44**, 917 (1965).
[17] D. J. Gauthier, M. S. Malcuit, and R. W. Boyd, Phys. Rev. Lett. **61**, 1827 (1988).